

West-East High Speed Flow Field Conference
19-22, November 2007
Moscow, Russia

NUMERICAL SIMULATION OF NONSTATIONARY VISCOUS FLOWS BASED ON QUASI-GASDYNAMIC EQUATIONS

T. G. Elizarova

*Institute for Mathematical Modeling, Russian Academy of Sciences, Miusskaya pl. 4a,
Moscow, 125047, Russia*

E-mail: telizar@mai.ru, web page: <http://www.imamod.ru/~elizar>

Key words: quasi-gasdynamical equations, numerical simulation, nonstationary gas flows

Abstract. Numerical algorithm for calculation of non-stationary viscous gasdynamic flows is presented. Algorithm is based on the quasi-gasdynamical equation system, that can be regarded as the special form of regularization in Navier-Stokes equations, including the additional dissipative terms. Examples of the numerical calculations are reported.

1. QUASI-GASDYNAMIC EQUATION SYSTEM

In this paper the contemporary mathematical model - the quasi-gasdynamical (QGD) system of equations - and the related numerical methods are reported. QGD model generalizes the Navier-Stokes (NS) system of equations but differs from the NS system by additional dissipative terms with a small multiplicative parameter τ . The first variants of the QGD system were presented in, e.g. ^{1,2} and developed later in, e.g. ³⁻⁶.

Equations for description of gasdynamic flows in the local form can be presented as the equations for conservation of mass, momentum and total energy

$$\frac{\partial \rho}{\partial t} + \operatorname{div} \vec{j}_m = 0, \quad (1)$$

$$\frac{\partial(\rho \vec{u})}{\partial t} + \operatorname{div}(\vec{j}_m \otimes \vec{u}) + \vec{\nabla} p = \operatorname{div} \Pi, \quad (2)$$

$$\frac{\partial}{\partial t} \left[\rho \left(\frac{\vec{u}^2}{2} + \varepsilon \right) \right] + \operatorname{div} \left[\vec{j}_m \left(\frac{\vec{u}^2}{2} + \varepsilon + \frac{p}{\rho} \right) \right] + \operatorname{div} \vec{q} = \operatorname{div}(\Pi \cdot \vec{u}), \quad (3)$$

and the entropy balance equation

$$\frac{\partial(\rho s)}{\partial t} + \operatorname{div}(\vec{j}_m s) = -\operatorname{div} \left(\frac{\vec{q}}{T} \right) + X, \quad (4)$$

where $X \geq 0$ is the nonnegative entropy production. Here the common notations are used. It is supposed that the entropy equation (4) is a sequence of the conservation

equations (1) – (3). Here ρ is the density, \vec{u} is the velocity-vector, $p = \rho\mathcal{R}T/\mathcal{M}$ is the pressure, \mathcal{M} is the molar mass, \mathcal{R} is the perfect-gas constant, T is the temperature, $\varepsilon = p/(\rho(\gamma - 1))$ is the internal energy, γ is the specific heat ratio. To close the system, the mass flux vector \vec{j}_m , the shear-stress tensor Π , and the heat flux vector \vec{q} must be expressed as a function of macroscopic flow quantities and their space derivatives.

If the gasdynamic variables ρ , \vec{u} and E are defined as instantaneous space-averaged quantities by physically infinity small volume, then the system (1) – (3) becomes the Navier-Stokes (NS) system that is closed by $\vec{j}_m = \rho\vec{u}$, $\Pi = \Pi_{NS}$, $\vec{q} = \vec{q}_{NS}$.

If the gasdynamic quantities are defined by means of time-space averaging, the system (1) – (3) can be closed by the quasi-gasdynamic (QGD) approach, e.g. ³⁻⁶. In the absence of the external forces the closing relations are

$$\vec{j}_m = \rho(\vec{u} - \vec{w}), \quad \text{where} \quad \vec{w} = \frac{\tau}{\rho}[\text{div}(\rho\vec{u} \otimes \vec{u}) + \vec{\nabla}p], \quad (5)$$

$$\Pi = \Pi_{NS} + \tau\vec{u} \otimes [\rho(\vec{u} \cdot \vec{\nabla})\vec{u} + \vec{\nabla}p] + \tau I [(\vec{u} \cdot \vec{\nabla})p + \gamma p \text{div}\vec{u}], \quad (6)$$

$$\vec{q} = -\kappa\vec{\nabla}T - \tau\rho\vec{u} \left[(\vec{u} \cdot \vec{\nabla})\varepsilon + p(\vec{u} \cdot \vec{\nabla})\left(\frac{1}{\rho}\right) \right]. \quad (7)$$

Here μ and κ are the viscosity and heat conductivity coefficients, respectively, τ is a small parameter, that has the dimension of time. For the perfect gas it may be calculated as $\tau = \mu/pSc$, where Sc is the Schmidt number. The resulting equation system (1) – (7) must be completed by the state equations for the perfect gas and the expressions for μ and κ coefficients.

The equation system (1) – (7) is completed by the initial and boundary conditions. In contrast to the NS system, continuity equation (1) in the QGD system is an equation of a second order in space. So the QGD system must be completed by an additional boundary condition. This condition for pressure p is obtained by imposing appropriate boundary condition for mass flux vector \vec{j}_m .

The QGD and the NS systems differ by the space derivative terms of the order of $O(\tau)$. It was shown³ that for stationary flows, the dissipative terms (terms in τ) in the QGD equations have the asymptotic order of $O(\tau^2)$ for $\tau \rightarrow 0$. In the boundary layer limit both QGD and NS equations reduce to the Prandtl equation system.

For perfect gas the entropy production for the QGD system is the entropy production for the NS system completed by the additional terms in τ , that are the squared left-hand sides of the classical stationary Euler equations with positive coefficients:

$$\begin{aligned} X = & \kappa \left(\frac{\vec{\nabla}T}{T} \right)^2 + \frac{(\Pi_{NS} : \Pi_{NS})}{2\mu T} + \frac{p\tau}{\rho^2 T} \left[\text{div}(\rho\vec{u}) \right]^2 + \\ & + \frac{\tau}{\rho T} \left[\rho(\vec{u} \cdot \vec{\nabla})\vec{u} + \vec{\nabla}p \right]^2 + \frac{\tau}{\rho\varepsilon T} \left[\rho(\vec{u} \cdot \vec{\nabla})\varepsilon + p \text{div}\vec{u} \right]^2. \end{aligned} \quad (8)$$

Others gas dynamic models with nonclassical continuity equation are presented in, e.g.,^{7–12}. Models^{7–11} do not include the velocity derivatives in mass flux vector. The system¹² includes the second time derivatives, that do not appeared in the QGD model.

Terms in τ allow to construct the family of the novel numerical algorithms for simulation nonstationary supersonic and subsonic gasdynamic flows. The QGD algorithms inherit mathematical properties of the QGD system. They are efficient in code implementation by virtue of the directly "built in" τ -regularization, ensuring a high quality of the numerical solution.

2. FINITE-DIFFERENCE APPROXIMATION AND NUMERICAL ALGORITHMS FOR SUPERSONIC FLOWS

The finite-difference approximation of the QGD system is constructed in a flux form using the control volume method. The mass flux vector \vec{j}_m , the shear-stress tensor Π and the heat flux vector q , are implied, corresponding to conservation laws for the QGD equations (1) – (7). It makes the numerical algorithm compact and economic. Invariant form of the QGD system allows to construct the numerical methods for any orthogonal coordinate system for structured and unstructured space grids. The similar approximations are used for rectangular structural grids and for unstructured three-cornered grids⁶.

To solve the problem numerically, a grid in space and in time is introduced in a computational domain. All gas dynamic parameters – density ρ , pressure p and velocity \vec{u} are determined at the nodes of the computational grid. The values of gas dynamic parameters at the nodes with half-integer indices and at the cell's centers are determined as the arithmetic means of their values at the adjacent nodes.

An initial-boundary value problem is solved by applying an explicit in time finite-difference scheme. The spatial derivatives are approximated by the central differences with a second-order accuracy, and the time derivatives are approximated by the forward differences with a first-order accuracy.

To ensure a stability of a numerical solution for supersonic flows the term proportional to a grid step h is added to τ . Than, coefficient τ , viscosity and heat conductivity are calculated as

$$\tau = \frac{\mu}{pSc} + \alpha \frac{h}{c}, \quad \mu = \tau pSc, \quad \kappa = \gamma \mathcal{R} \frac{\tau pSc}{Pr(\gamma - 1)}, \quad (9)$$

where $c = \sqrt{\gamma \mathcal{R} T}$ is the local sound velocity, γ is the specific heat ratio, α is a numerical factor $0 \leq \alpha \leq 1$.

The time step is chosen with Courant stability condition $\Delta t = \beta h / c_{max}$, where the numerical coefficient $0 < \beta < 1$ is chosen according to the stability of the solution along the computations.

As a first example of application we consider a strong discontinuity step evolution problem in non-viscous gas without heat conductivity. It means that we solve Euler equations with artificial dissipation that is introduced as $\tau = \alpha h / c$. The initial-value problem is solved in the space interval $0 \leq x \leq 200$ for the time interval $0 \leq t \leq 8$.

We take $Sc = 1.$, $Pr = 2/3$ and $\gamma = 5/3$. The initial conditions form a discontinuity at $x = 100$. The values to the left and to the right from the break look as follows:

$$\rho(x, 0) = \begin{cases} 8, & x \leq 100 \\ 1, & x > 100 \end{cases}, \quad p(x, 0) = \begin{cases} 480, & x \leq 100 \\ 1, & x > 100 \end{cases}, \quad u(x, 0) = 0.$$

We used grid steps $h = 1, 0.5, 0.25, 0.125, 0.0625$ and 0.03125 with $\Delta t = 0.002$ for

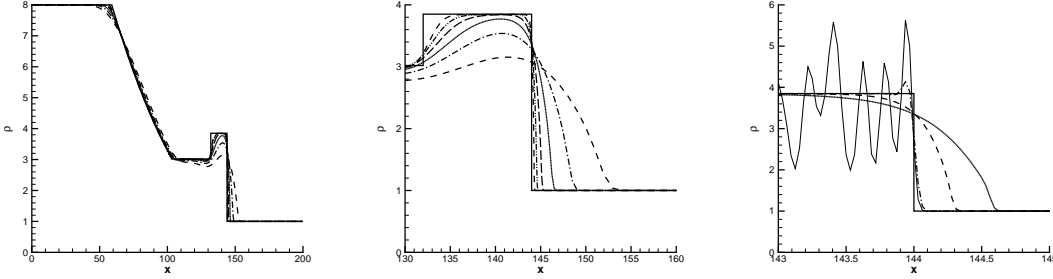


Figure 1: Density distribution along x (left - whole computational domain, right - fragments)

the first three variants, and $\Delta t = 0.0002$ for the last three ones. Convergency of the numerical results to analytical solution with reducing h for $t = 4$ is seen in Fig. 1 for $\alpha = 0.5$ (two left figures). The dependence of the solution from parameter α ($h = 0.03125$) is shown on the right figure for $\alpha = 1., 0.1, 0.5, 0.1$ and 0.02 . The last value corresponds to the "saw" solution, where numerical instability is clearly seen. The best solution is attained for $\alpha \sim 0.2 - 0.5$, $\beta \sim 0.1$.

3. NUMERICAL ALGORITHMS FOR SUBSONIC FLOWS AND THE KARMAN STREET CALCULATION

In contrast to a previous case (9), for calculations of subsonic flows the additional stabilizing term $\alpha h/c$ is introduced only in τ coefficient as

$$\tau = \frac{\mu_0}{pSc} \left(\frac{T}{T_0} \right)^\omega + \alpha \frac{h}{c}, \quad \mu = \mu_0 \left(\frac{T}{T_0} \right)^\omega, \quad \kappa = \mu \frac{\gamma \mathcal{R}}{Pr(\gamma - 1)}.$$

In this case the heat flux and the shear-stress tensor are not affected by the grid dissipation.

Within a framework of the QGD model the simple unreflecting boundary conditions may be applied on the free subsonic boundaries. They are similar to those used for viscous incompressible flows. For inlet boundary (in) they have a form

$$\frac{\partial p}{\partial n} = \alpha_{in}, \quad \vec{u} = \vec{u}_{in}, \quad \rho = \rho_{in},$$

where $\alpha_{in} \sim 1/Re$ is a small constant, n is a unity vector normal to the boundary. At the outlet boundary (out) soft boundary conditions are imposed for density and

velocity, but pressure supposed to be constant:

$$\frac{\partial \rho}{\partial n} = 0, \quad \frac{\partial \vec{u}}{\partial n} = 0, \quad p = p_{out}.$$

As an example a numerical simulation of a flow in a vicinity of a circular cylinder for Mach number $Ma = 0.1$ and Reynolds number $Re = 90$ is presented. This problem is a well known test, e.g.¹³, and the citations therein. Calculations were made for air flow, $\gamma = 1.4$, $Pr = 0.72$, $Sc = 0.746$, and $\omega = 0.74$, using unstructured grid consisting from 2191 points. Here $\alpha = 0.1$. In Fig. 2 time dependence of the velocity is shown. Calculated Strouhal number is $Sh=0.147$. Rayleigh formula for incompressible flow gives $Sh = 0.212(1 - 21.2/Re) = 0.162$, that corresponds to $\sim 10\%$ of the accuracy of grid definition for cylinder diameter. With the grid refinement the numerical result converges to the experiment prediction.

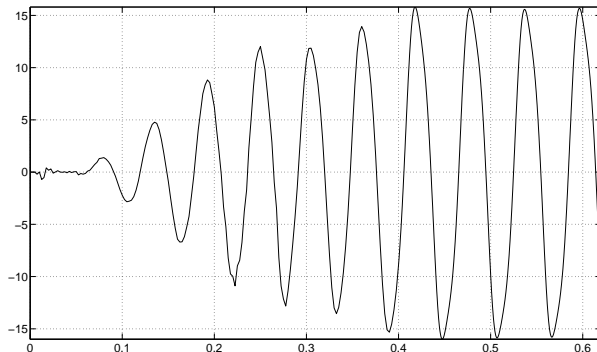


Figure 2: Time-dependence for u_y in a cylinder wake.

In Fig.3 Karman street in the wake is plotted using isolines for \vec{u}^2 in dimensional form ($u_{in} = 35, 31$ m/sec, and cylinder diameter $D=0.3$ m.).

Numerical experiments show, that the computational time for one time-step in QGD algorithm is equal to the computational time in solving the NS equations by applying the similar method - the central-difference scheme explicit in time.

4. LAMINAR-TURBULENT TRANSITION IN BACKWARD-FACING STEP CALCULATION

We calculate the flow in a plane channel of length L and height $2H$ with a backward-facing step of height H for $L = 30H$. The flow is characterized by Reynolds and Mach numbers

$$Re = \frac{\rho_0 U_0 H}{\mu_0}, \quad Ma = \frac{U_0}{c_0}, \quad (10)$$

with a density ρ_0 and temperature T_0 at inlet, where $U_0 = \int u_x dy$ is the mean entrance velocity. The channel boundaries are supposed to be adiabatic with no-slip and non-penetrating boundary conditions. The Poiseuille velocity profile and the non-reflecting boundary conditions are imposed at the entrance and exit boundaries.

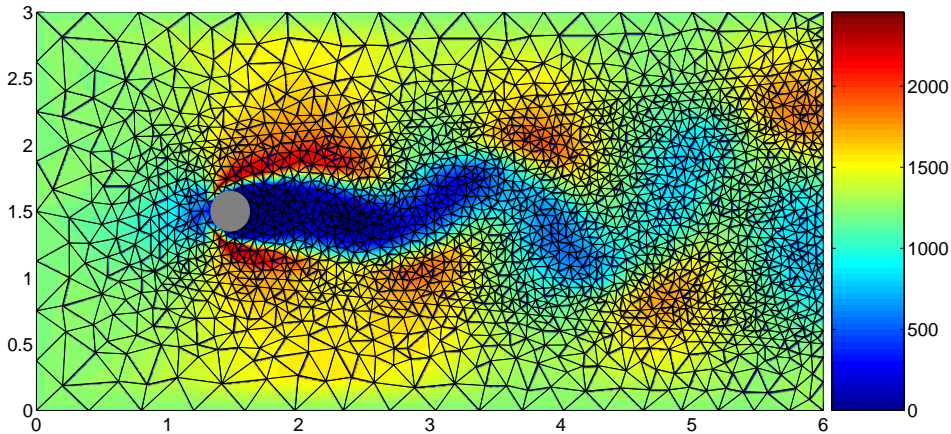


Figure 3: Mesh and flow picture for non-stationary flow near a cylinder, $Re = 90$.

Gas flow with $u_x = u_y = 0$, $\rho = \rho_0$, $T = T_0$ was taken as the initial condition. Calculations were done for the air flow with $\gamma = 1.4$, $Pr = 0.737$, $Sc = 0.746$, and $\omega = 0.74$, the using uniform rectangular cells with $h = 0.1, 0.05, 0.03$ in 2D computational domain. The results for $Ma = 0.1$ are presented below.

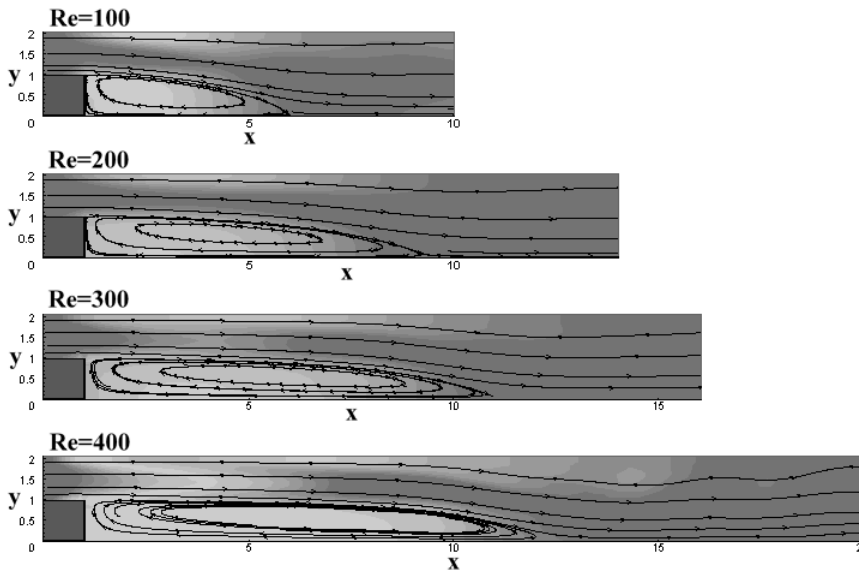


Figure 4: Density and stream functions for $Re= 100, 200, 300$ and 400 . $Ma = 0.1$

According to e.g.¹⁴, the length of the separation zone L_s increases almost linearly for increasing Reynolds number, than reaches a maximum value, and finally it decreases. The increasing part is related with a laminar flow regime, and the decreasing part is related with the development of flow instabilities leading to a turbulent regime.

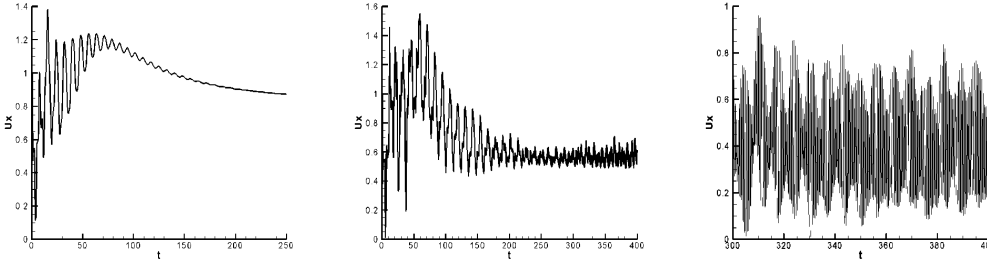


Figure 5: Time-evolution of u_x for $Re = 300, Re = 600$ and $Re = 1000$.

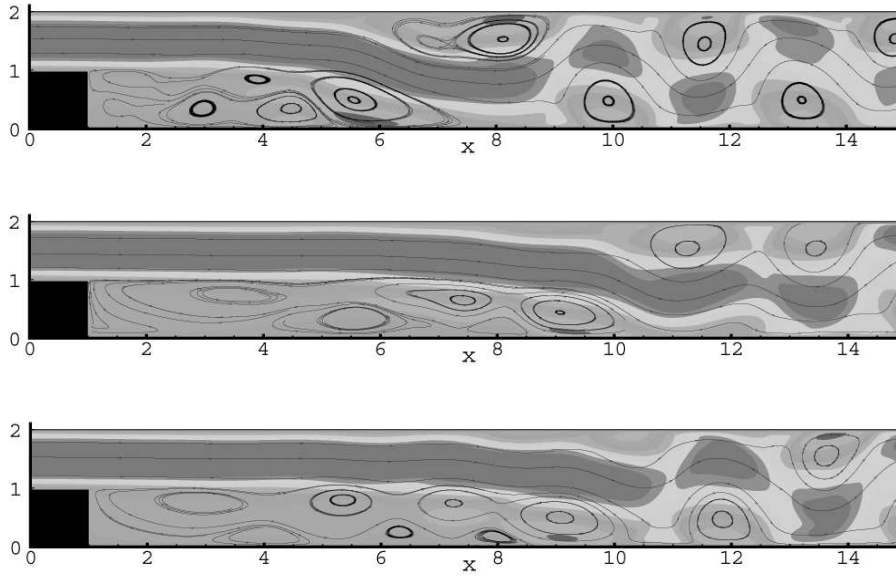


Figure 6: Simultaneous stream function and velocity isolines u_x for $Re = 1000, t = 80, t = 360, t = 400, \alpha = 0.3$, fragments

For small Reynolds numbers (laminar regime) the numerical calculations lead to a stationary flow, and the results are in a good agreement with the NS numerical modeling and with experiment. Here terms in τ do not affect the NS solution and act as a numerical regularizator. The steady state flow pictures for $Re=100, 200, 300$ and 400 are shown in fig.4. These results correspond to $h=0.05, \alpha = 0.5$ and $\beta = 0.3$. Evolution of the velocity at $Re = 300, 600$ and 1000 are shown in fig.5. The onset of non-stationary flow is shown for $Re=600$.

For increasing values of Re , the flow becomes strongly non-stationary and the length of the separation zone must be found by time-averaging. Here the terms in τ become important and act as a subgrid turbulent dissipation. Fig.6 shows a set of instantaneous flow pictures for $Re = 1000, h=0.03, \alpha = 0.3$ and $\beta=0.5$. In fig.7 the corresponding time-average picture is presented.

In fig.8 calculated values of the length L_s (normalized in H) of the recirculation zone behind a step are compared with the experimental values¹⁴, where Re was based on a length $\sim 2H$). It shows a reasonable agreement between computation

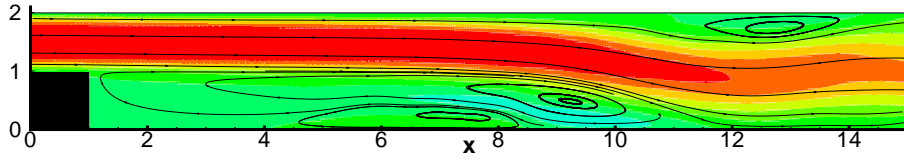


Figure 7: Stream function for averaged flow, $Re = 1000$, fragment.

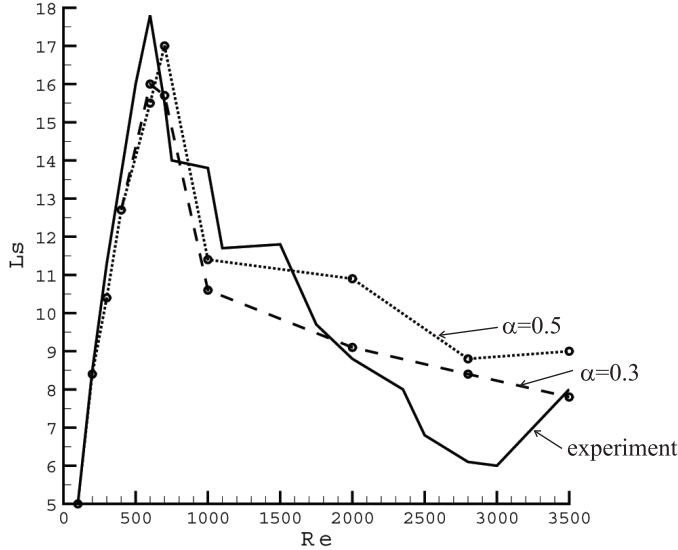


Figure 8: Separation zone length. Dash-lines - calculations, full line - data⁷.

and experiment both for laminar regimes and for non-developed turbulent regimes, including the point of bifurcation. The non-monotonous behavior of L_s for $Re > 1000$ could be related with an the onset of three-dimensional structures in the flow that cannot be simulated in a present 2D modeling.

5. CONCLUSIONS

Contemporary mathematical model for gas flow simulations, named the quasi-gas-dynamic (QGD) equation system, is presented. The QGD equations differ from the Navier–Stokes system by the additional dissipative terms with a small multiplicative parameter. Basing on the QGD model the new robust algorithms for non-stationary viscous flow simulations are constructed and verified.

The present computations of a backward-facing step flow show that the QGD model provides a numerical simulation for both laminar and turbulent flows, including the transition between these regimes. Even in the 2D formulation the present model allows to simulate the main features of the flow. The simple structure of the present algorithm is well suited for 3D numerical computations which implies parallel computing.

The QGD model employs a unified computational algorithm with only one free

parameter. The advantages of the model follow from the validity of the basic fluid dynamic conservation laws, well established for the QGD equation system.

References

- [1] T.G.Elizarova and B.N.Chetverushkin, "Kinetic algorithms for calculating gas-dynamic flows", *Comput. Mathem. and Mathem. Phys*, 25 164-169 (1985), 164–169.
- [2] B.N.Chetverushkin, *Kinetic-consistent schemes in gasdynamics*, Moscow, MGU, 1999 (in Russian).
- [3] Yu.V.Sheretov, *Numerical simulation of liquid and gas flow based on quasi-hydrodynamic and quasi-gasdynamical equations*, Tver, TGU, 2000 (in Russian).
- [4] T.G.Elizarova and Yu.V.Sheretov, "Theoretical and numerical investigation of quasi-gasdynamical and quasi-hydrodynamic equations", *Comput. Mathem. and Mathem. Phys*, 41 (2001), 219–234.
- [5] T.G.Elizarova, M.E.Sokolova and Yu.V. Sheretov, "Quasi-gasdynamical equations and numerical simulation of viscous gas flows", *Comput. Mathem. and Mathem. Phys*, 45, 524 - 534 (2005).
- [6] T.G.Elizarova, *Quasi-gasdynamical equations and numerical methods for viscous flow computations*, Scientific World, Moscow, 2007 (in Russian).
- [7] N.A.Slezkin, "About a differential equations of a gas motion", *Dokl. of USSR Ac. of Science*, 77, 205–208 (1951)
- [8] S.V.Vallander, "Equations of viscose gas motion", *Dokl. Of USSR Ac. of Science*, 58 25–27 (1951)
- [9] Yu.L.Klimontovich, "About the necessity and possibility of unified description of kinetical and hydrodynamical processes", *Theoretical and Mathematical Physics*, 92 312-330 (1992)
- [10] H.Brenner, "Navier–Stokes revisited", *Physica A*, 349 60–132 (2005)
- [11] H.C. Ottinger, *Beyond equilibrium thermodynamics*, Hoboken: John Wiley, 2005.
- [12] B.V. Alexeev, *Generalized Boltzmann physical kinetics*, Elsevier, Amsterdam, 2004.
- [13] P. Roushan, X.L. Wu, "Universal wake structures of Karman vortex streets in two-dimentional flows", *Physics of Fluids*, 17 073601 (2005)
- [14] B.F. Armaly, F. Durst, J.C.F. Pereira and B. Schonung, "Experimental and theoretical investigation of backward-facing step flow", *J. of Fluid Mech*, 127, 473-496 (1983).